ISSN 0915-633X

NATIONAL INSTITUTE FOR FUSION SCIENCE

Configurational Effects on Low Collision Plasma Confinement in CHS Heliotron/Torsatron

M.F.Heyn, S.V. Kasilof, W. Kernbichler, K. Matsuoka,
V.V. Nemov, S. Okamura, O.S. Pavlichenko

(Received - Dec. 26, 2000)

NIFS-675 Jan. 2001

RESEARCH REPORT
NIFS Series

TOKI, JAPAN

Configurational Effects on Low Collision Plasma Confinement in CHS Heliotron/Torsatron

M.F.Heyn[***], S.V.Kasilov[**], W.Kernbichler[***], K.Matsuoka[*], V.V.Nemov[**], S.Okamura[*], O.S.Pavlichenko[**]

[*]*National Institute for Fusion Science, Toki, Japan*
[**]*Institute of Plasma Physics, NSC KIPT, Kharkov, Ukraine*
[***]*Institut für Theoretische Physik, Technische Universität Graz, Graz, Austria*

Abstract

Multihelicity effects on low collisionality (~1/ν) regime of neoclassical transport has been analyzed for full range of magnetic field configurations of CHS Heliotron/Torsatron. Transport coefficients for this regime has been calculated according to an approach developed in [5]. It was shown that the drift-orbit-optimized configuration of CHS device [6] has the best confinement properties for low collision plasma confinement.

[1] Introduction

CHS device is an *l=2, m=8* low aspect ratio (R/a≈5) Heliotron/Torsatron with a flexible magnetic field configuration. Changing of poloidal field configuration ensures the configuration flexibility of CHS. The variety of configurations with different rotational transform and shear profiles, magnetic well and helical ripple can be obtained with different plasma equilibrium/stability/confinement properties.

The advanced scenario of the wall conditioning and plasma fueling/heating at moderate heating power (P_{ECH}≤0.5MW, P_{NBI}≤1 MW) resulted in achievement of plasma with temperatures of both electrons and ions in the range of 1 KeV at plasma density of 1-2.10^{13} cm^{-3} in CHS. In such conditions both electrons and ions enter in low collisionality regime of neoclassical transport. The relevance of neoclassical theory to experimental results on CHS was discussed in [1-4]. In the 1/ν regime the configurational effects on neoclassical transport coefficients are manifested through different radial profiles of magnetic field ripple structure. The small aspect ratio helical device CHS is characterized by a rather rich spectrum of magnetic field harmonics of comparable amplitude (Fig.1). The neoclassical values of the electron heat diffusivity for CHS were calculated for single helicity magnetic field model [2]. As for the approach of calculation of transport coefficients using a single helicity model of stellarator field is non-adequate, multi-helicity effects of the magnetic field configuration were taken into account in the 1/ν regime by introducing the form factor accounting these effects. This approach was used at the ion heat diffusivity calculations for CHS [3].

In this report we present results of calculation of neoclassical transport in low collisionality regime for full range of configurational space of CHS. These studies use an approach for low collisionality transport calculation proposed in [5].

[2] Neoclassical plasma transport in CHS.

In stellarators for the low collisional frequency transport there is a number of different regimes depending on the particle collision frequency, electric field and other parameters. For these regimes rather convenient analytical descriptions can be realized [8]. However for the transition regions between these regimes, the analytical description is more complicated. For practical estimates, it is convenient to have analytical formulas, which are valid with reasonable accuracy in all regions of particle collision frequencies, without complications related to the transition regions. Formulas (4) and (12) of [7] are often used for this purpose. We also used these equations with some revisions based, in particular, on the results obtained in [5].

The particle flux density for single helicity model stellarator field has the following form [7]:

$$\Gamma_n^{na} = -\varepsilon_t^2 \sqrt{\varepsilon_h} \nu_d^2 n_a \int_0^\infty dx x^{5/2} e^{-x} \frac{\widetilde{\nu}_a(x)}{\omega_a^2(x)} A_a(x) \qquad (1)$$

with

$$\omega_a^2(x) = 3\widetilde{\nu}_a^2(x) + \frac{\varepsilon_t}{\varepsilon_h}\left(1.67(\omega_E + \omega_{Ba})^2 + \left(\frac{\varepsilon_t}{\varepsilon_h}\right)^{1/2}\left[\frac{1}{4}\omega_{Ba}^2 + 0.6|\omega_{Ba}|\widetilde{\nu}_a\left(\frac{\varepsilon_h}{\varepsilon_t}\right)^{3/2}\right]\right), \qquad (2)$$

$$\widetilde{\nu}_a(x) = \frac{\nu_a}{\varepsilon_h x^{3/2}}, x = \frac{w}{T_a}, \omega_E = \frac{1}{rB}\frac{\partial \Phi}{\partial r}, \omega_{Ba} = -\frac{T_a}{Z_a erB}\frac{\partial \varepsilon_h}{\partial r} x, \nu_{da} = -\frac{T_a}{Z_a erB},$$

$$A_a(x) = \frac{1}{n_a}\frac{\partial n_a}{\partial r} + \frac{Z_a e}{T_a}\frac{\partial \Phi}{\partial r} + \left(x - \frac{3}{2}\right)\frac{1}{T_a}\frac{\partial T_a}{\partial r}.$$

The different terms in (2) reflect existence of different collision frequency regions and radial electric field. If the first term in (2) dominates, so called 1/ν regime is realized.

The general approach for calculation of transport coefficients in the 1/ν regime taking into account the real configuration of magnetic field in stellarator was developed in [5]. In this method the neoclassical transport coefficients are calculated by integration along the magnetic field line. Such integration takes into account the particles trapped within one magnetic field period and those that are trapped within several field periods as well. If the magnetic field is originally available in real-space coordinates calculations can be performed without a field transformation to magnetic coordinates. In accordance with [5] particle flux densities (averaged over a magnetic surface) can be presented in the form:

$$\Gamma_n = -\frac{\sqrt{8}}{9\pi^{3/2}} \frac{v_T^2 \rho_L^2}{\nu R^2} \varepsilon_{eff}^{3/2} \int_0^\infty \frac{dz e^{-z} z^{5/2}}{A(z)} \frac{n}{f_0} \frac{\partial f_0}{\partial r} \qquad (3)$$

$$\varepsilon_{eff}^{3/2} = \frac{\pi R^2}{8\sqrt{2}} \lim_{L_s \to \infty} \left(\int_0^{L_s} \frac{ds}{B} \right) \left(\int_0^{L_s} \frac{ds}{B} |\nabla \psi| \right)^{-2} \int_{B_{min}^{(abs)}/B_0}^{B_{max}^{(abs)}/B_0} db' \sum_{j=1}^{j_{max}} \frac{\hat{H}_j^2}{\hat{I}_j}, \qquad (4)$$

$$\hat{H}_j = \frac{1}{b'} \int_{s_j^{(min)}}^{s_j^{(max)}} \frac{ds}{B} \sqrt{b' - \frac{B}{B_0}} \left(4\frac{B_0}{B} - \frac{1}{b'} \right) |\nabla \psi| k_G, \quad \hat{I}_j = \int_{s_j^{(min)}}^{s_j^{(max)}} \frac{ds}{B} \sqrt{1 - \frac{B}{B_0 b'}}. \qquad (5)$$

Here, f_0 is the Maxwellian distribution (as a function of the particle energy w and the magnetic surfaces ψ), $v_T = \sqrt{2T/m}$ is the thermal velocity, $\rho_L = mcv_T/(eB_0)$ is the typical Larmor radius, $A(z)$ is a quantity related to the collision operator ($A(z) = \frac{3\sqrt{\pi}}{4}(\eta + \eta' - \frac{\eta}{2z})$, $\eta(z) = \int_0^z \exp(-x)\sqrt{x}dx$), R is the major radius of the torus, $\partial f_0/\partial r$ is the average normal derivative, $k_G = (\mathbf{h}\times(\mathbf{h}\cdot\nabla)\mathbf{h})\cdot\nabla\psi/|\nabla\psi|$ is the geodesic curvature of the magnetic field line ($\mathbf{h}=\mathbf{B}/B$). The integral over z in (3) is general for any magnetic configuration and corresponds to the integration over w. The characteristic features of the specific magnetic field geometry manifest themselves through the factor ε_{eff}, where ε_{eff} is the effective ripple modulation amplitude. This factor naturally takes into account contribution to the 1/ν transport arising from all classes of trapped particles, i.e. particles trapped not only within one magnetic field period but also within several magnetic field periods. The quantity ε_{eff} is calculated by integration over magnetic field line length, L_s, (within the sufficiently large interval of $0 \div L_s$) and over the perpendicular adiabatic invariant of trapped particles (by means of the variable b', $B_{min}^{(abs)}$ and $B_{max}^{(abs)}$ are the minimum and maximum values of B within the interval of $0 \div L_s$). The quantities $s_j^{(min)}$ and $s_j^{(max)}$ in the sum over j in (5) correspond to the turning points of trapped particles. The result (3) differs from the corresponding formula for the standard stellarator [8] by a simple replacement of the helical modulation amplitude ε_h (along the magnetic field line) through the ε_{eff} quantity. Therefore, for any magnetic configuration the 1/ν transport coefficients can be obtained from the corresponding coefficients for the standard stellarator with the replacement of ε_h by ε_{eff}.

For most regimes of CHS one can't neglect other terms in (2). Let us discuss the question of calculation of transport for CHS specific magnetic field geometry.

It should be remembered that the decrease of the asymmetric long-mean-free-path transport for any regime is directly connected with a decrease of the trapped particle orbit displacement from the flux surface Δr_n, or, more exactly, with a decrease of the bounce averaged particle drift velocity across a magnetic surface, $v_{an} = \Delta r_n / \tau_b$ (τ_b is the bounce period). It follows from the neoclassical transport theory that a decrease in v_{an} leads to a decrease of asymmetric neoclassical transport in all regimes and that in all regimes the transport coefficients scale with v_{an}^2. In equation (1) this is shown by the presence of the factor ε_t^2. As it follows from [5] for the 1/ν regime the decrease in transport corresponds to a decrease of factor $\varepsilon_{eff}^{3/2}$. Therefore the decrease of v_{an}^2 can be taken into account in (1) by defining the factor L as

$$L = \frac{\varepsilon_{eff}^{3/2}}{\varepsilon_h^{3/2}} \qquad (6)$$

(up to the accuracy determined by the pitch angle scattering frequency used in [8]).

In fact, the decrease of L corresponds to the decrease of the v_{an}^2 which is averaged over pitch

angles with a weight specific for the confinement regime. To estimate the factor L in the presence of a radial electric field for the condition $\nu_a / \varepsilon_h < |\omega_E|$ one should bear in mind that for this condition the main contribution to the neoclassical transport comes from the helically trapped particle fraction in a relatively narrow region of pitch angles near the transition region between different classes of trapped particles [8] . The ν_{an}^2 value for these trapped particles may differ from the one which is averaged over pitch angles and which corresponds to the quantity (6). Nevertheless here we shall use an assumption about the equality of these two ν_{an}^2 values (as it is realized, e.g., for the standard stellarator magnetic field [8]) and use quantity L as a form-factor accounting the specific geometry of magnetic field in CHS for low collisional transport calculations also in the condition $\nu_a / \varepsilon_h < |\omega_E|$.

[3] Configurational effects of transport in CHS.

Configurational space of CHS was characterized by one parameter R_{ax} where R_{ax} indicates the magnetic axis position in the φ=0 plane. This position was changed (as in experiment) by changing of the compensating coil currents.

Calculations of ε_{eff} were performed for 3 configurations: 1) so called drift-orbit-optimized configuration [6] (R_{ax}=87.7 cm); 2) standard configuration (R_{ax}=92.1 cm) and 3) outward shifted configuration (R_{ax}=100 cm). The magnetic field produced by a helical winding current was computed with the use of the Biot-Savar law for the helical conductor modeled with 8 filaments in 3 layers (2+3+3, from the inner side of the conductor). The distribution of the filaments was roughly uniform within of conductor cross section. Calculations were performed over the interval L_s corresponding to 250 magnetic field periods. Figs. 2-4 illustrate results of these calculations for all 3 configurations. Note that small islands for the rotational transform ι=1 are not shown on Fig.2 and the island surface in Fig.3 corresponds to ι=4/5.

The results of ε_h and ε_{eff} computations for configurations 1) and 2) are shown in Fig.5. The results of $\varepsilon_{eff}^{3/2}$ computations for all 3 configurations are shown in Fig.6.

From the results follows that for the standard configuration of CHS for the magnetic surfaces at moderate distances from the magnetic axis (0.5<r/a<1) the $\varepsilon_{eff}^{3/2}$ value is greater (by a factor up to 2) than that for the standard stellarator. For the drift-orbit-optimized configuration the $\varepsilon_{eff}^{3/2}$ value turns out to be approximately by a factor of 10 smaller than the value for the standard stellarator. As pointed out in [6] this configuration is very close to the omnigenuous configuration and, therefore, has improved confinement of locally trapped particles. Our results give a qualitative evaluation of corresponding improvement of plasma transport.

We also obtained simple analytical approximations for effective ripple coefficient ε_{eff} and rotational transform ι as functions of magnetic axis position R_{ax} (Appendix I). They can be used for interpolation of data on ε_{eff} and ι in the region of R_{ax} = 87.7-100 cm.

ACKNOWLEDGMENT

This work was partly supported by the "Monbusho International Scientific Research Program: Joint Research" (Japan) and by the Association EURATOM-OEAW under contract ERB 5004 CT 96 0020

REFERENCES

[1] K.Ida, M.Osakabe at al., 17th IAEA Fusion Conference, Yokohama (1998), IAEA-CN-69/EX2/2

[2] S.Okamura, K.Matsuoka at al., 17th IAEA Fusion Conference, Yokohama (1998), IAEA-CN-69/OV4/5

[3] K.Ida, M. Osakabe at al., Nuclear Fusion **39**, 1649 (1999).

[4] M.F.Heyn, S.V.Kasilov et al., XII International Conference on Stellarators, Madison (1999)

[5] V.V.Nemov, S.V.Kasilov et al., Phys Plasmas **6**, 4622 (1999)

[6] S.Okamura, K.Matsuoka et al., Annual Report of NIFS (April 1996-March 1997), 225 (1997)

[7] D.E.Hastings, W.A.Houlberg and K.C.Shaing, Nucl. Fusion **25**, 445 (1985)

[8] A.A. Galeev and R.Z. Sagdeev, in *Voprosy Teorii Plazmy* (Atomizdat, Moscow, 1973), No. 7, p.205 (in Russian); A.A. Galeev and R.Z. Sagdeev, *Reviews in Plasma Physics*, edited by M.A. Leontovich (Consultants Bureau, New York, 1979), Vol.7, p.257.

APPENDIX I

Interpolation of rotational transform ι(r/a) and effective ripple modulation amplitude ε_{eff} in the range of R_{ax} =87.7 –100 cm for CHS can be calculated from the next formulas:

```
IOTA(X)=1.0/(AIOTA+BIOTA*X**CIOTA)

AIOTA=-254.08606+5.463299*rax-0.028972158* rax
**2.0
BIOTA=287.55786-6.1595955* rax +0.03270849* rax
**2.0
CIOTA=158.4092-3.3598228* rax +0.017942902* rax
**2.0
EPSH(X)=AEPSH/(1.0+BEPSH*EXP(-CEPSH*X))
```

AEPSH=13.263028-0.15140422* rax
BEPSH=43016.912-922.17493* rax +4.9121912* rax **2.0
CEPSH=-221.5679+4.8387577* rax -0.025899053* rax **2.0

$\varepsilon_{eff}^{3/2}$

In these formulas X- normalized magnetic surface radius r/a (a-radius of last closed magnetic surface), rax = R_{ax} (cm) - the magnetic axis position in the φ=0 plane, IOTA–rotational transform, EPSH -

Figure Captions

Fig.1 Rotational transform and harmonics of magnetic field in CHS (standard configuration)

Fig. 2 Magnetic surfaces (a) and mod B along magnetic field line (b) for drift-orbit-optimized configuration of CHS

Fig.3 Magnetic surfaces (a) and mod B along magnetic field line (b) for standard configuration of CHS

Fig.4 Magnetic surfaces (a) and mod B along magnetic field line (b) for outward shifted configuration of CHS

Fig.5 ε_h and ε_{eff} radial profiles for standard (a) and drift-orbit-optimized (b) configurations.

Fig.6 $\varepsilon_{eff}^{3/2}$ versus normalized radius for CHS configurations (1- drift-orbit-optimized; 2 – standard; 3 – outward shifted)

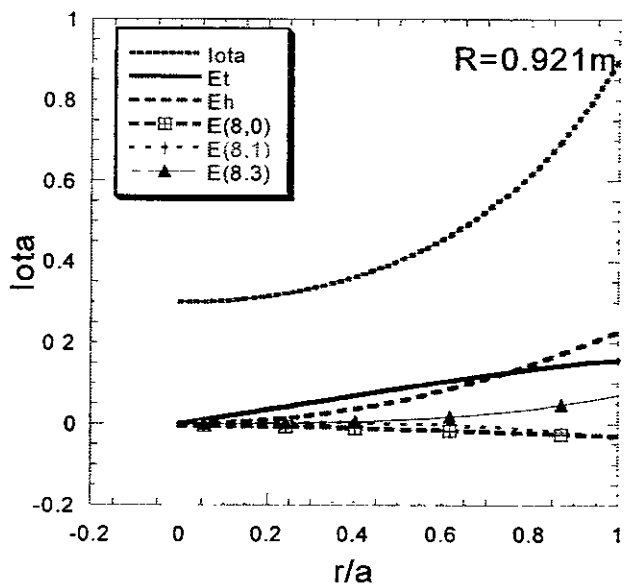

Fig.1

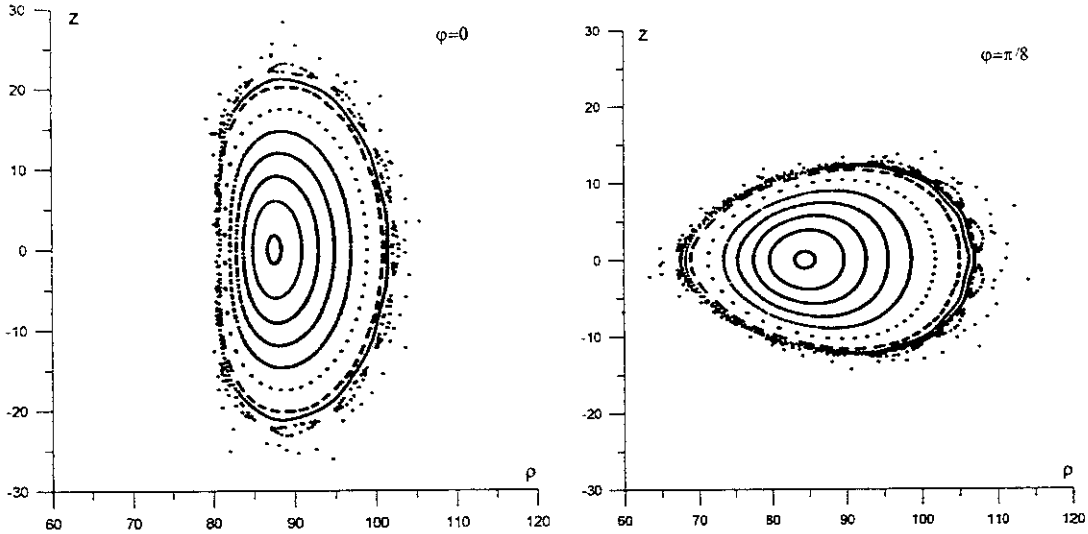
z
φ=0
ρ
z
φ=π/8
ρ

a)

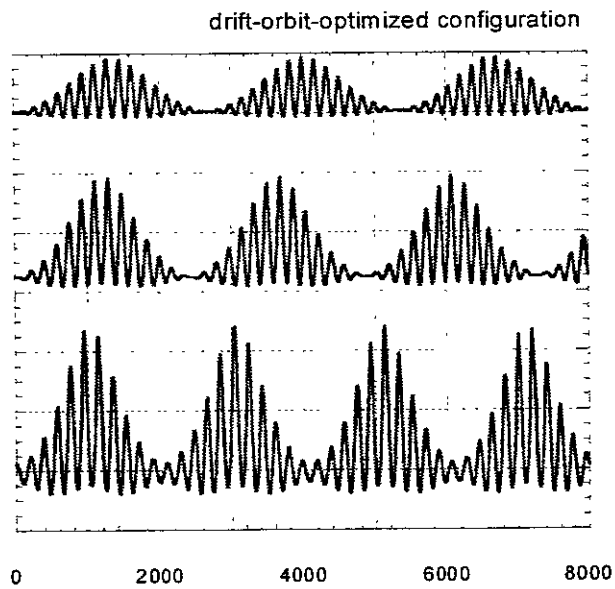
drift-orbit-optimized configuration
0
2000
4000
6000
8000

b)

Fig.2

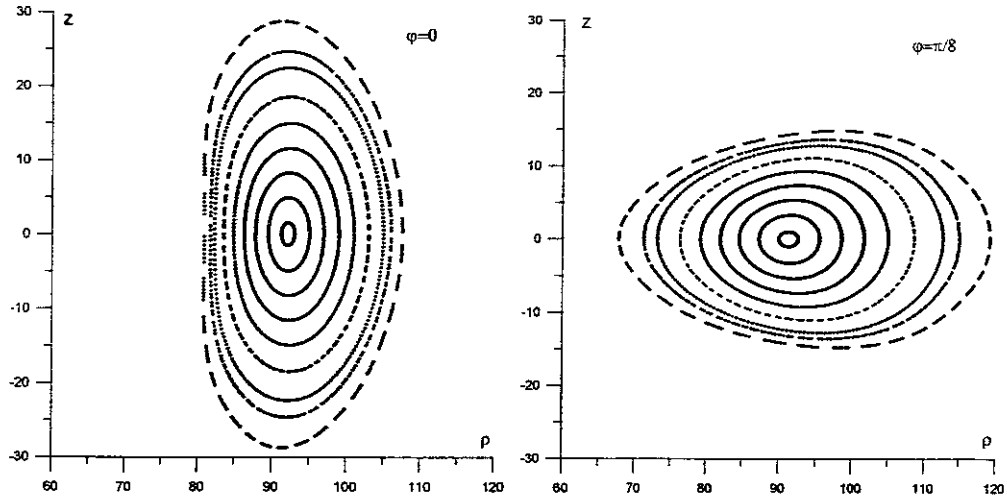
z
φ=0
ρ
z
φ=π/8
ρ

a)

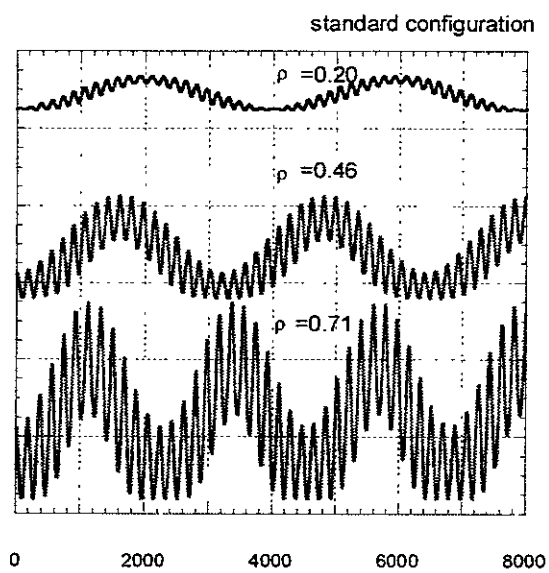
standard configuration
ρ =0.20
ρ =0.46
ρ =0.71
0
2000
4000
6000
8000

b)

Fig.3

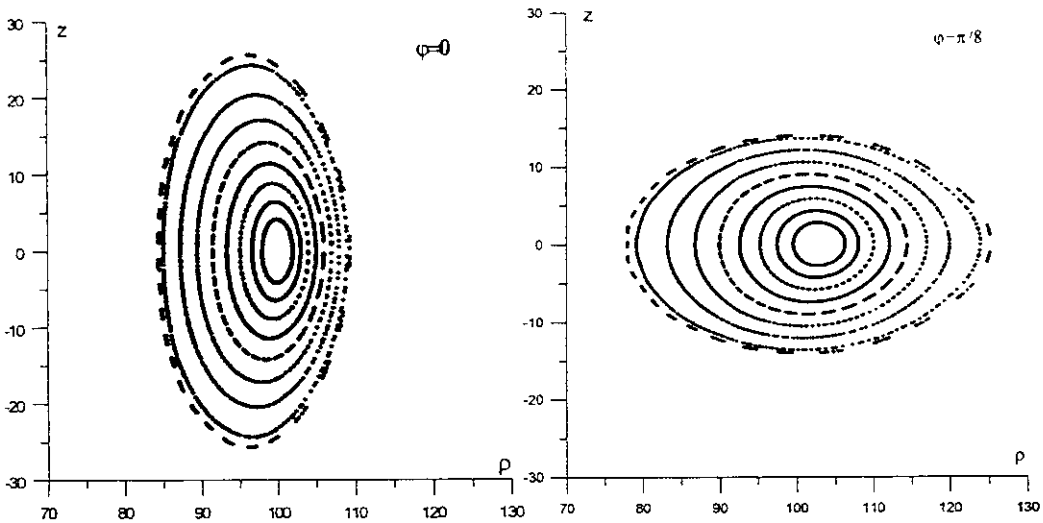

a)

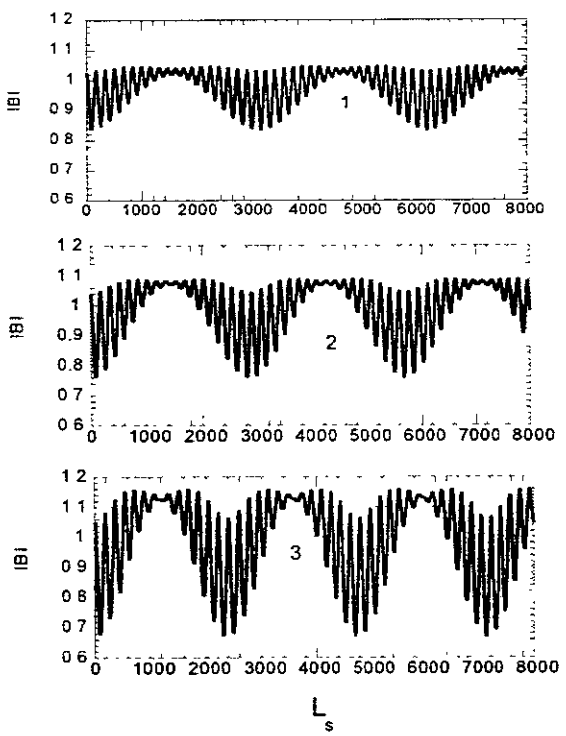

b)

Fig.4

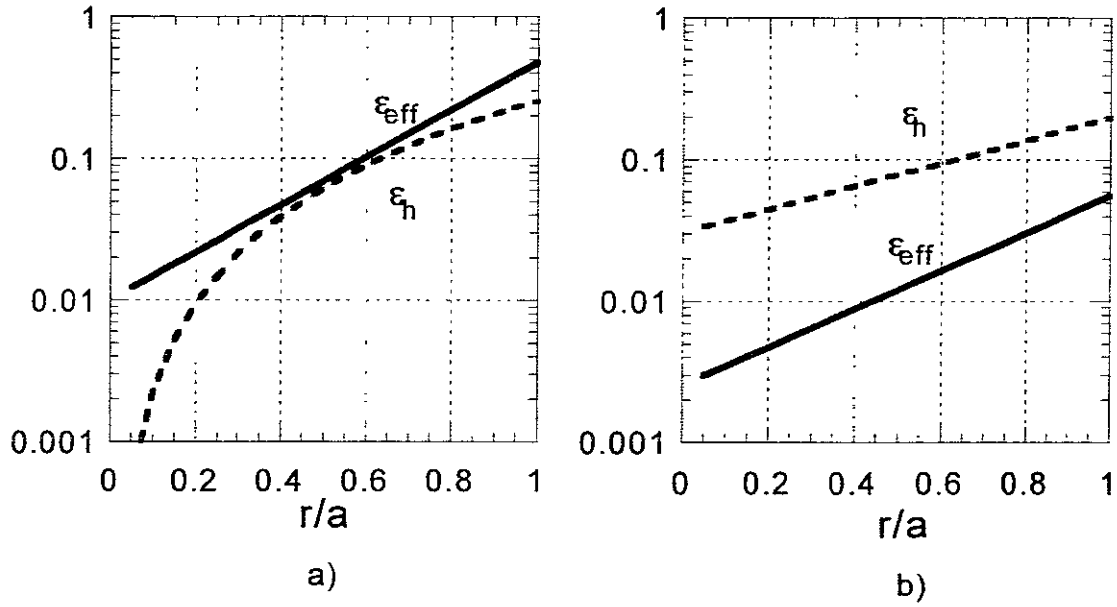
1
0.1
0.01
0.001
0
0.2
0.4
0.6
0.8
1
r/a
ε_{eff}
ε_h
a)
b)

Fig.5.

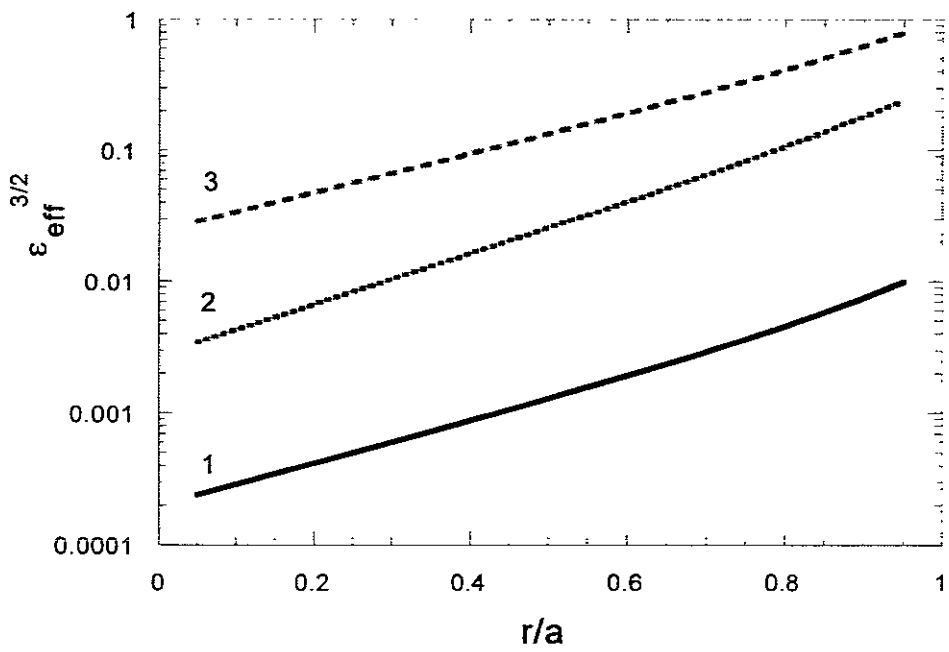
1
0.1
0.01
0.001
0.0001
0
0.2
0.4
0.6
0.8
1
r/a
$\varepsilon_{eff}^{3/2}$
3
2
1

Fig.6

Recent Issues of NIFS Series

NIFS-658 B J Peterson, Y Nakamura, K Yamazaki N Noda, J Rice Y Takeiri M Goto, K Narihara, K Tanaka K Sato S Masuzaki S Sakakibara, K Ida, H Funaba, M Shoji, M Osakabe, M Sato, Yuhong Xu T Kobuchi N Ashikawa, P deVries M Emoto H Idei K Ikeda, S Inagaki, N Inoue, M Isobe, S Kado K Khlopenkov S Kubo R Kumazawa, T Minami, J Miyazawa T Morisaki, S Murakami S Muto, T Mutoh Y Nagayama, H Nakanishi, K Nishimura, T Notake, Y Liang, S Ohdachi, Y Oka, T Ozaki, R O Pavlichenko, A Sagara, K Saito, R Sakamoto, H Sasao, M Sasao, T Seki, T Shimozuma, H Suzuki, M Takechi, N Tamura, K Toi T Tokuzawa, Y Torii, K Tsumori, I Yamada, S Yamaguchi, S Yamamoto, M Yokoyama, Y Yoshimura, K Y Watanabe, T Watari, K Kawahata, O Kaneko, N Ohyabu, H Yamada, A Komori, S Sudo, O Motojima
Impurity transport induced oscillations in LHD Sep 2000
(IAEA-CN-77/EXP5/27)

NIFS-659 T Satow, S Imagawa, N Yanagi, K Takahata, T Mito, S Yamada, H Chikaraishi, A Nishimura, I Ohtake, Y Nakamura, S Satoh, O Motojima,
Achieved Capability of the Superconducting Magnet system for the Large Helical Device Sep 2000
(IAEA-CN-77/FTP1/15)

NIFS-660 T Watari, T Mutoh, R Kumazawa, T Seki, K Saito, Y Torii Y P Zhao , D Hartmann , H Idei, S Kubo, K Ohkubo, M Sato, T Shimozuma, Y Yoshimura, K Ikeda, O Kaneko, Y Oka, M Osakabe, Y Takeiri, K Tsumori, N Ashikawa P C deVries, M Emoto, A Fukuyama , H Funaba, M Goto K Ida, S Inagaki, N Inoue, M Isobe, K Itoh, S Kado, K Kawahata, T Kobuchi, K Khlopenkov, A Komori, A Krasilnikov , Y Liang,S Masuzaki, K. Matsuoka, T Minami, J Miyazawa, T Morisaki, S Morita, S Murakami, S. Muto, Y Nagayama, Y Nakamura, H Nakanishi, K Narihara, K. Nishimura, N Noda, A TNotake, S Ohdachi N Ohyabu, H Okada , M Okamoto, T Ozaki, R O Pavlichenko B J Peterson, A Sagara, S Sakakibara, R Sakamoto, H Sasao, M Sasao K Sato, S Satoh, T Satow, M Shoji, S Sudo, H Suzuki, M Takechi, N Tamura ,S Tanahashi, K Tanaka, K Toi, T Tokuzawa, K Y Watanabe, T Watanabe, H Yamada, I Yamada, S Yamaguchi, S Yamamoto, K Yamazaki, M Yokoyama, Y Hamada, O Motojima, M Fujiwara,
The Performance of ICRF Heated Plasmas in LHD Sep 2000
(IAEA-CN-77/EX8/4)

NIFS-661 K Yamazaki, K. Y Watanabe, A Sagara, H Yamada, S Sakakibara, K Narihara, K Tanaka, M Osakabe, K Nishimura, O Motojima, M Fujiwara, the LHD Group,
Helical Reactor Design Studies Based on New Confinement Scalings Sep 2000
(IAEA-CN-77/ FTP 2/12)

NIFS-662 T Hayashi, N Mizuguchi, H Miura and T Sato,
Dynamics of Relaxation Phenomena in Spherical Tokamak Sep 2000
(IAEA-CN-77THP2/13)

NIFS-663 H. Nakamura and T Sato, H. Kambe and K Sawada and T Saiki,
Design and Optimization of Tapered Structure of Near-field Fiber Probe Based on FDTD Simulation Oct 2000

NIFS-664 N Nakajima
Three Dimensional Ideal MHD Stability Analysis in L=2 Heliotron Systems Oct 2000

NIFS-665 S Fujiwara and T Sato,
Structure Formation of a Single Polymer Chain I Growth of trans Domains Nov 2000

NIFS-666 S Kida,
Vortical Structure of Turbulence Nov 2000

NIFS-667 H Nakamura, S Fujiwara and T Sato,
Rigidity of Orientationally Ordered Domains of Short Chain Molecules Nov 2000

NIFS-668 T Mutoh, R Kumazawa, T Seki, K Saito, Y Torii, F. Shimpo, G Nomura, T Watari, D A Hartmann, M Yokota, K Akaishi, N. Ashikawa, P deVries, M Emoto, H Funaba, M. Goto, K Ida, H Idei, K. Ikeda, S Inagaki, N Inoue, M Isobe, O Kaneko, K Kawahata, A Komori, T Kobuchi, S Kubo, S Masuzaki, T Morisaki, S Morita, J Miyazawa, S Murakami, T Minami, S Muto, Y Nagayama, Y Nakamura, H Nakanishi, K Narihara, N. Noda K Nishimura, K Ohkubo, N Ohyabu, S Ohdachi, Y Oka, M. Osakabe, T Ozaki, B.J Peterson, A Sagara, N Sato, S Sakakibara, R Sakamoto, H Sasao, M Sasao, M Sato, T Shimozuma, M Shoji, S Sudo, H Suzuki, Y Takeiri, K Tanaka, K Toi, T Tokuzawa, K Tsumori, K Y Watanabe T Watanabe, H Yamada, I Yamada, S Yamaguchi, K Yamazaki, M Yokoyama, Y Yoshimura, Y Hamada, O Motojima, M Fujiwara,
Fast- and Slow-Wave Heating of Ion Cyclotron Range of Frequencies in the Large Helical Device Nov 2000

NIFS-669 K Mima, M S. Jovanovic, Y. Sentoku, Z-M Sheng, M M Skoric and T Sato,
Stimulated Photon Cascade and Condensate in Relativistic Laser-plasma Interaction Nov 2000

NIFS-670 L Hadzievski, M M. Skoric and T Sato,
On Origin and Dynamics of the Discrete NLS Equation Nov 2000

NIFS-671 K Ohkubo, S. Kubo, H Idei, T Shimozuma, Y Yoshimura, F. Leuterer M Sato and Y. Takita,
Analysis of Oversized Sliding Waveguide by Mode Matching and Multi-Mode Network Theory Dec 2000

NIFS-672 C Das, S Kida and S Goto,
Overall Self-Similar Decay of Two-Dimensional Tirbulence Dec 2000

NIFS-673 L A Bureyeva, T Kato, VS Lisitsa and C Namba,
Quasiclassical Representation of Autoionization Decay Rates in Parabolic Coordinates Dec 2000

NIFS-674 L A. Bureyeva, VS Lisitsa and C Namba,
Radiative Cascade Due to Dielectronic Recombination Dec 2000

NIFS-675 M F Heyn S V Kasilof, W Kernbichler, K Matsuoka, V V Nemov, S Okamura, O S Pavlichenko,
Configurational Effects on Low Collision Plasma Confinement in CHS Heliotron/Torsatron, Jan 2001